Original Article

Molecular dynamics simulations of thermal transport in hybrid silicene-graphane nanoribbons

Marjune T. Bonilla[1,2,*], and Giovanni J. Paylaga[2,*]

[1]*University of Science and Technology of Southern Philippines-Panaon Campus, Punta, Panaon, Misamis Occidental, 7205, Philippines*
[2]*Physics Department, Mindanao State University – Iligan Institute of Technology A. Bonifacio Avenue, 9200 Iligan City, Philippines*

**Corresponding author: marjune.bonilla@ustp.edu.ph; giovanni.paylaga@g.msuiit.edu.ph*

Received: 20 Jun. 2025 || Revised: 25 Feb. 2026 || Accepted: 28 May 2026 || Available Online: 26 Nov. 2026

How to cite:
Bonilla MT, Paylaga GJ. 2026. Molecular dynamics simulations of thermal transport in hybrid silicene-graphane nanoribbons. The Palawan Scientist. 18(2):in press. https://doi.org/10.69721/TPS.J.2026.18.2.12

UNCORRECTED PROOF

ABSTRACT

The distinctive properties of silicene and graphane motivate their integration into a novel heterostructure with tunable interface-dependent electronic, magnetic, and thermal characteristics for silicon-compatible nanoelectronic and thermal-rectification applications. This pioneering study investigates thermal transport in hybrid silicene-graphane nanoribbons — a less-explored heterostructure compared with silicene-graphene systems with applications in silicon-compatible nanoscale devices. Unlike zero-gap graphene or MoS_2, which was a fixed gap of approximately 1.8 eV, silicene-graphane leverages graphane's insulating nature and interface/strain effects for tunable bandgaps, enabling room-temperature field-effect transistor operation and enhanced performance. Non-equilibrium molecular dynamics simulations using the Large Atomic/Molecular Massively Parallel Simulator (LAMMPS) employed Nosé-Hoover thermostats and Tersoff/AIREBO potentials to model silicene-graphane nanoribbons. The Green-Kubo method was used to calculate thermal conductivity; hot/cold edge baths drove steady-state heat flux. At 300 Kelvin, silicene showed a thermal conductivity of 20.42 W/m·K, compared with graphane's unexpectedly high value of 1592.89 W/m·K. Conductivity decreased with temperature due to Umklapp scattering from anharmonic vibrations. Kapitza resistance at the silicene-graphane interface was 1.39×10^{-10} m^2·K/W (ΔT=9.7 K) and 7.04×10^{-11} m^2·K/W (ΔT=4.9 K), matching typical 2D heterostructure values (10^{-10}–10^{-9} m^2·K/W). These values reflect phonon mismatch under bidirectional flux (±1.0 eV/ps) in the 40 × 5 nm

©2026, Western Philippines University

system. These findings illuminate anisotropic transport, enhancing hybrid nanoribbons' role in tailored nanodevice thermal management.

Keywords: kapitza resistance, non-equilibrium molecular dynamics, thermal conductivity, thermal transport, umklapp scattering

INTRODUCTION

Two-dimensional monolayer honeycomb structures of graphene, boron nitride, and silicon offer remarkable properties and are promising materials for future applications (Topsakal et al. 2010). Graphene is a monolayer sheet of graphite or a two-dimensional honeycomb lattice of sp^2 bonded carbon, which has attracted considerable attention due to its unique and exceptional electronic and chemical properties (Mbayachi et al. 2021). The thermal properties of graphene are promising for thermal transport and heat management in nanoelectronic devices. Studies have revealed that graphene has an ultrahigh thermal conductivity even higher than that of carbon nanotubes, suggesting that it is a good candidate for heat management in nanoelectronic devices (Rajabpour et al. 2011).

Hydrogenation can be utilized to cover a graphene ribbon totally or partially to construct structures with controllable properties. One of these structures is called graphane, which is a single sheet of graphene fully adsorbed with hydrogen atoms, with each carbon atom bonded to a hydrogen atom alternately on either side of the layer (Wu and Yang 2012). Graphane shares the same two-dimensional honeycomb structure as graphene, but its saturated carbon skeleton gives rise to a bandgap and therefore provides more possibilities for the development of novel carbon-based semiconductors (Li et al. 2025). Graphane was also theoretically proposed (Sofo et al. 2007) and experimentally synthesized (Singh and Yakobson 2009) by selectively hydrogenating graphene nanoribbons and transforming the bond type between carbon atoms from sp^2 to sp^3. It has special electrical, mechanical, and thermal properties (Sofo et al. 2007) and it can attain a permanent magnetic moment through hydrogen vacancies (Topsakal et al. 2010). Silicene has also started to attract the attention of scientist in materials science because of its electronic properties (Xiang-Tao et al. 2013). Silicene is a one-atom-thick, two-dimensional crystal of silicon with a hexagonal lattice structure that is related to that of graphene but with atomic bonds that are buckled rather than flat (Tsai et al. 2013). Silicene has a buckled structure owing to the large ionic radius of silicon, which creates new possibilities for manipulating the dispersion of electrons and controlling the band gap electrically in silicene (Xiang-Tao et al. 2013).

UNCORRECTED PROOF

©2026, Western Philippines University

The unusual properties of silicene and graphane motivate researchers to introduce a new heterostructure material, which may exhibit interesting characteristics suitable for nanoelectronic devices in future applications. The researchers decided to create a new hybrid structure combining the silicene and graphane nanoribbons. This new hybrid heterostructure material, called silicene-graphane nanoribbon, is conceptually similar to the graphene-graphane nanoribbon studied by Rajabpour et al. (2011). The researchers chose silicene as a replacement for graphene since the structure and properties of silicene are almost the same as those of graphene. In addition, silicene can be easily integrated into the existing silicon-based nanotechnology. The novelty of this study lies in its first-time focus on hybrid silicene-graphane nanoribbons for thermal transport, distinguishing it from prior silicene-graphene work (Zhou et al. 2022). The silicene-graphane nanoribbon may possess interesting electronic and magnetic properties and may have a wide range of applications in nanostructured devices for the near future. These properties might also be strongly dependent on the interface between the silicene and graphane nanoribbons. Perhaps, these structures with intrinsic thermal asymmetries will provide an aopportunity to investigate the possibility of introducing a promising thermal rectifier, similar to recently proposed thermal rectifiers such as graphene-graphane nanoribbons (Rajabpour et al. 2011), silicon-carbon nanotube interfaces (Zhang et al. 2013) and multi-walled carbon nanotubes (Gordiz et al. 2011).

Silicene-graphane heterostructures show promise for advanced electronics. Silicene, a buckled silicon analog of graphene, enables tunable bandgaps through buckling modulation or applied strain/electric fields, as predicted by ab initio calculations. These mechanisms open gaps up to approximately 0.5 eV or more, supporting field-effect transistors (FETs) with ambipolar transport—meaning both electron and hole conduction—similar to graphene but with silicon-like compatibility for complementary metal–oxide–semiconductor (CMOS) integration. While silicene-graphene heterostructures exist (e.g., for thermal transport), silicene-graphane (hydrogenated graphene) combinations are less explored but are theoretically consistent with bandgap tuning via strain or interface effects in 2D heterobilayers. Graphane's insulating nature could enhance silicene's gap control, aiding FET performance. They offer advantages like silicon compatibility and room-temperature operation over graphene (zero gap) or MoS_2 (fixed gap of approximately1.8 eV gap) (Zhou et al. 2022; Grazianetti et al. 2023). Thermal rectification is a phenomenon in which thermal transport along a specific axis is dependent upon the sign of the temperature gradient or heat current (Roberts and Walker 2011). It is also an important nonlinear and asymmetric thermal transport phenomenon in which heat is regulated to transfer more preferentially in one direction than the

©2026, Western Philippines University

UNCORRECTED PROOF

other (Shrestha et al 2020). The scope of this study centers on using molecular dynamics (MD) simulations to characterize thermal transport properties in hybrid silicene-graphane nanoribbons, building on their potential for nanoelectronic and thermal management applications. The study also aims to investigate whether the Kapitza effect occurs at the interface of the silicene-graphane nanoribbons by simulating the heat flux and temperature profiles. Molecular dynamics (MD) simulations are a cornerstone of research on thermal transport in nanoscale 2D materials like hybrid silicene-graphane nanoribbons. Molecular dynamics simulations model atomic trajectories by solving Newton's equations with empirical potentials, capturing phonon-mediated heat flow in complex heterostructures where silicene's buckling and graphane's hydrogenation create asymmetric transport paths. This directly probes thermal conductivity (κ), rectification ratios, and length/size effects in nanoribbons, inaccessible via continuum models. Molecular dynamics simulations excel in modelling hybrid systems because they can handle large supercells (10^3-10^6 atoms), anharmonicities, and non-equilibrium conditions (NEMD) at finite temperatures (e.g., 300 Kelvin (K)), making them ideal for studying nanoribbons' finite-size scattering unlike infinite-sheet assumptions (Zhong 2021). In this paper, the study aimed to investigate the nature of thermal transport in hybrid silicene-graphane nanoribbons using the Large-scale Atomic/Molecular Massively Parallel Simulator (LAMMPS) package through NEMD simulations. Specifically, the study aimed to calculate the thermal conductivity of silicene and graphane nanoribbons across a range of temperatures, simulate the heat flux and corresponding temperature profiles for each nanoribbon type, and examine the presence of the Kapitza effect at the silicene-graphane nanoribbon interface by analyzing the interfacial temperature behavior under heat flux conditions.

METHODS

Flow Chart

The schematic diagram (flow chart) employed in this study is shown in Figure 1. To investigate thermal transport in silicene-graphane nanoribbons, the nanoribbon structures were first constructed using the Code::Blocks programming environment. Code::Blocks was used to programmatically construct the silicene, graphane, and silicene-graphane heterostructure. A for loop replicated the atomic basis of the system's zigzag chirality, as shown in Figure 2, enabling efficient generation of the 2D lattice model. Code::Blocks served as the integrated development environment (IDE) to write and compile C/C++ code for defining atomic coordinates. The for loop iterated over unit cell repetitions—typically nesting loops for the x/y directions in zigzag-edged silicene (Si atoms buckled above/below the plane) interfaced with graphane (hydrogenated graphene)—to build periodic

©2026, Western Philippines University

UNCORRECTED PROOF

supercells matching experimental lattice parameters. The constructed silicene, graphane, and silicene-graphane heterostructures were visualized and validated using HyperChem software (Hypercube Inc. 2007). HyperChem is a molecular modeling software package designed for computational chemistry simulations. It enables users to build, visualize, and analyze molecular structures in 3D. Moreover, the atomic coordinates from Code::Blocks were then imported into the Large Atomic/Molecular Massively Parallel Simulator (LAMMPS) environment (NTESS 2025) which was also used in the studies of Zhong (2021) and Dehaghani et al. (2022) to perform molecular dynamics simulations.

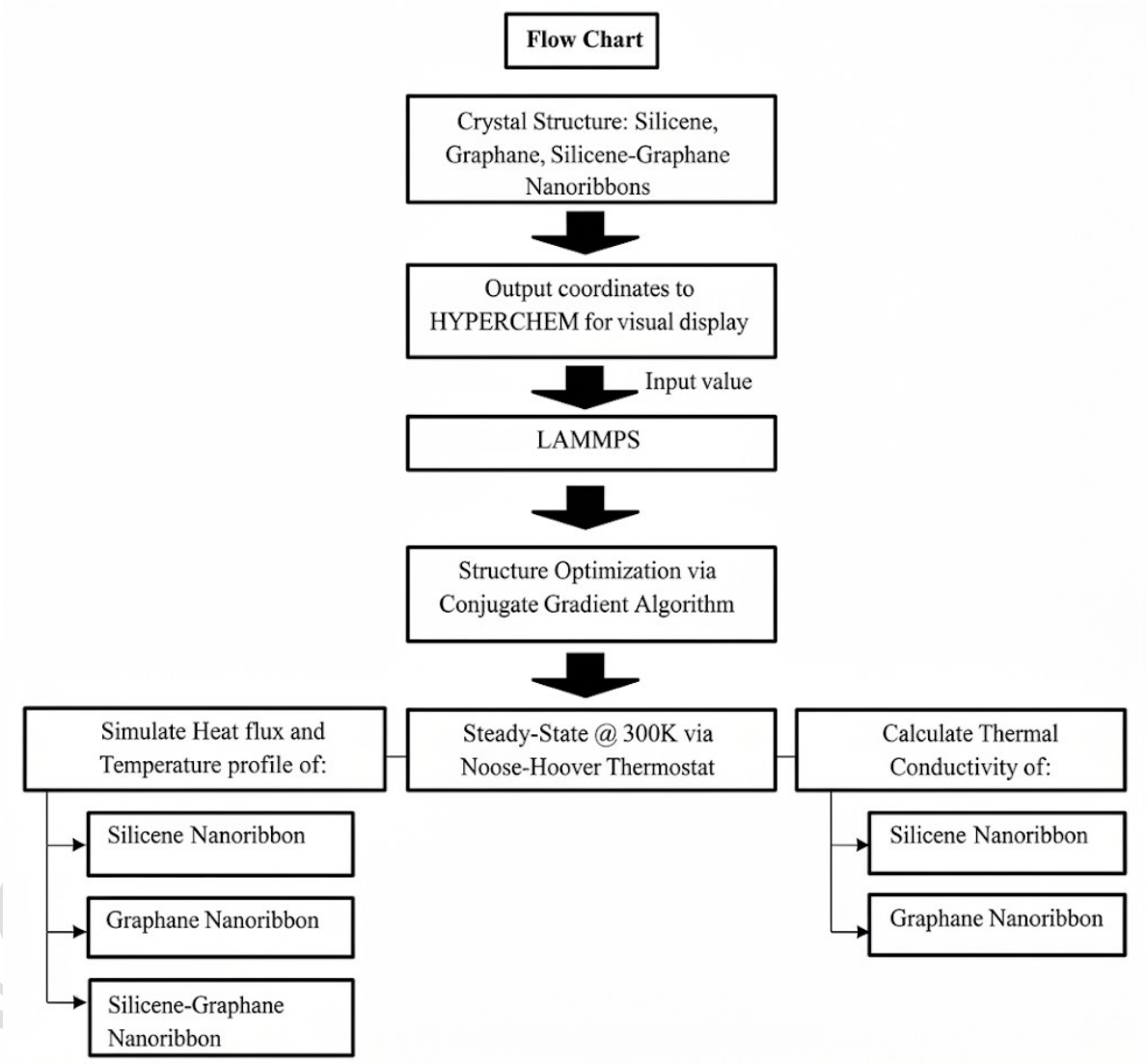
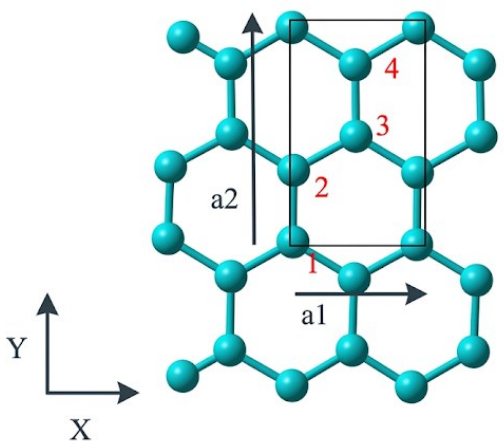


Figure 1. Schematic diagram (flow chart) employed in this study.

©2026, Western Philippines University



Basis atoms

	X	Y	Z
1	0.00	0.00	0.00)
2	0.00	a_0	0.00)
3	a1/2	a2/2	0.00)
4	a1/2	2.5 a_0	0.00)

Lattice vectors

a1: $\left(2\frac{\sqrt{3}}{2}a_0 \quad 0.00 \quad 0.00\right)$

a2: (0.00 $\quad 3\,a_0 \quad$ 0.00)

Figure 2. The orthogonal unit cell structure of the chosen atoms with bond length a_0. Atoms 1, 2, 3, and 4 are the chosen basis atoms, a1 and a2 are the lattice vectors.

Nanoribbon Structures

In constructing the silicene-graphane structure, the researchers selected four basis atoms (1, 2, 3, and 4) and manually determined the coordinates for each atom type. Figure 2 illustrates the orthogonal unit cell used to replicate the structure via its lattice vectors. The bond lengths (a_0) for Si-Si, C-C, and C-H bonds were 2.28 Å (CCCBD 2022), 1.53 Å, and 1.11 Å (Topsakal et al. 2010), respectively. The silicene and graphane nanoribbons each measured 20 nm in length and 5 nm in width. Furthermore, the silicene-graphane nanoribbon measured 40 nm × 5 nm.

Structures were constructed using the Code::Blocks program, following the parameters outlined in Figure 2. The code generated a nested loop over the four basis atoms of the zigzag chirality in the hexagonal structure: first along the x-axis (incrementing by the first lattice vector a1), then along the y-axis (incrementing by the second lattice vector a2). The resulting atomic coordinates were imported into HyperChem for 3D visualization and structural verification, with the resulting structures shown in Figures 3, 4, and 5.

UNCORRECTED PROOF

©2026, Western Philippines University

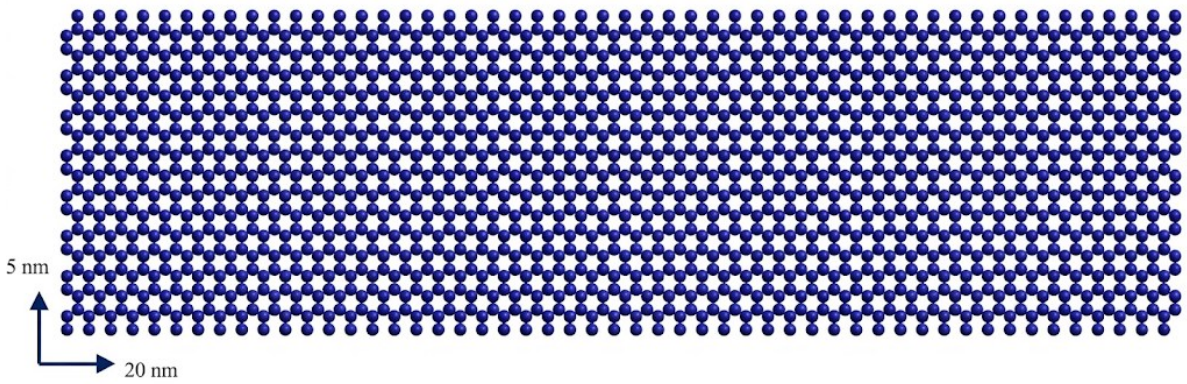


Figure 3. A 20 nm × 5 nm silicene nanoribbon composed of silicon (blue) atoms.

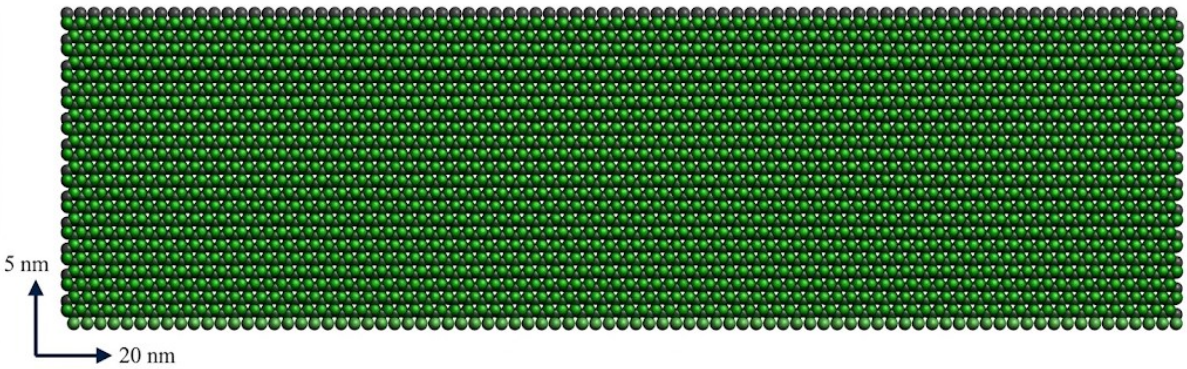


Figure 4. A 20 nm × 5 nm graphane nanoribbon composed of carbon (black) and hydrogen (green) atoms.

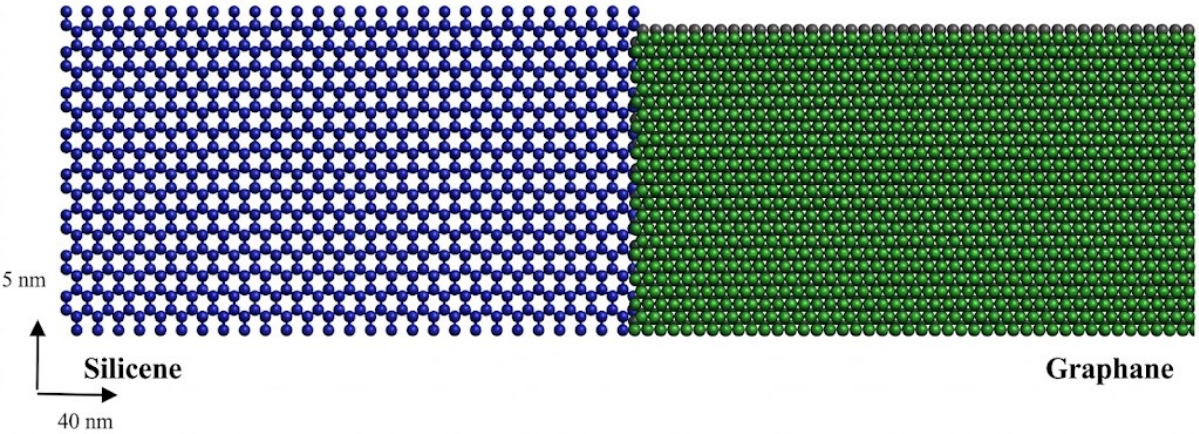


Figure 5. A 40 nm × 5 nm silicene-graphane nanoribbon composed of silicene (left side) and graphane (right side).

Steady State Procedure

The atomic coordinates generated by Code::Blocks were simulated in LAMMPS, a classical molecular dynamics code. The optimized structures of silicene, graphane, and silicene-graphane nanoribbons were obtained by applying a conjugate gradient algorithm (via the min_style cg and minimize commands). The optimized structures were then subjected to a Nose-Hoover thermostat (NPT/NVT ensembles) to reach a steady state at 300

©2026, Western Philippines University

K. Steady state refers to a condition in a system in which properties like temperature or heat flux remain constant over time, despite ongoing processes such as heat transfer. In thermal transport, steady state occurs when the temperature distribution does not change with time at any point, even as heat continuously flows through the material. Heat entering any section equals heat leaving it, creating a stable profile governed by Fourier's law: q = −kA dT/dx, where q is heat flux, k is thermal conductivity, A is area, and dT/dx is the temperature gradient (Fiveable 2026). Moreover, the parameters used in the steady state procedure were units (metal), atomic style, and input files (e.g., silicenecoor.txt for silicene coordinates). The optimization parameters included the conjugate gradient (CG) minimizer, tolerances 1.0e-15, max iterations 500,000 iterations. Equilibration was performed using the NPT ensemble at 300 K and 1.01325 GPa for 2,000 steps, followed by production runs of 2,000,000 steps for steady state. The boundary conditions were (p p p), the timestep was 0.001 ps, and the thermodynamic output intervals were also specified.

Thermal Conductivity

For the calculation of thermal conductivity (κ), the Green-Kubo method was utilized. This method uses a one-dimensional temperature profile, which is imposed on the simulation cell, and the corresponding heat flux is used to determine the thermal conductivity (Plimpton 1995). Mathematically, the thermal conductivity k_{MD} is expressed through the following equation:

$$k_{MD} = \frac{V}{3\,k_B T^2} \int < J(0) \cdot J(t) > dt \qquad (1)$$

where T is the temperature, k_B is the Boltzmann constant, V is the volume, and J is the heat flux.

Moreover, thermal conductivity was computed using the Green-Kubo formalism in LAMMPS via heat flux autocorrelation from equilibrated restart files (restart.300k.270000 for silicene; restart.300k.60000 for graphane) at 300 K. The parameters used were as follows: units (metal), correlation length p=2, sample interval s=1000, dump interval d=2000, timestep of 0.001 ps, boundary condition (p p p) and 10,000 production steps after reset_timestep 0. The following quantities were then computed: per-atom KE (myKE), PE (myPE), stress (myStress), and heat/flux (flux). The flux components Jx, Jy, and Jz were scaled by volume. The fix ave/correlate command was used to calculate the running autocorrelation of the flux vectors, which were saved in J0Jt.dat. Unit conversions (e.g., from $eV^2/ps/Å^2$ to W/mK via kB, eV2J, etc.) and trapezoidal integration using trap () were applied to calculate κii (i=1,2,3), with the average thermal conductivity, κ = (κ11+κ22+κ33)/3, reported alongside density.

©2026, Western Philippines University

UNCORRECTED PROOF

Heat Flux and Temperature Profile

Thermal transport was simulated via NEMD in LAMMPS using the direct heat flux method. Systems were loaded from steady-state restart files (restart.300k.2000000 for silicene; 3.1874000 for graphane) with periodic boundaries (p p p), atomic style, and metal units. Hot and cold regions were defined as slabs along the x-direction (silicene: 0-10 and 190-200; graphane: 0-30 and 170-200, both spanning y=0-50, infinite z) as shown in Figures 6 and 7. Heat was added/removed at 1.0/-1.0 eV/ps via fix heat on the hot/cold groups, with microcanonical ensemble NVE integration applied to all atoms (excluding neighbors within 2.0 Å cutoff). Per-atom kinetic temperature was computed as T=KE/1.5kB (kB = 8.617339e-5 eV/K), spatially averaged (500/1000/500000 over x-bins of 10 lattice units, running average) into tempprofile.txt. Runs totaled 500,000 timesteps after reset_timestep 0, with thermo outputs every 1000 steps. The interatomic potentials used were Tersoff (SiC.tersoff) for silicene and AIREBO (CH.airebo) for graphane.

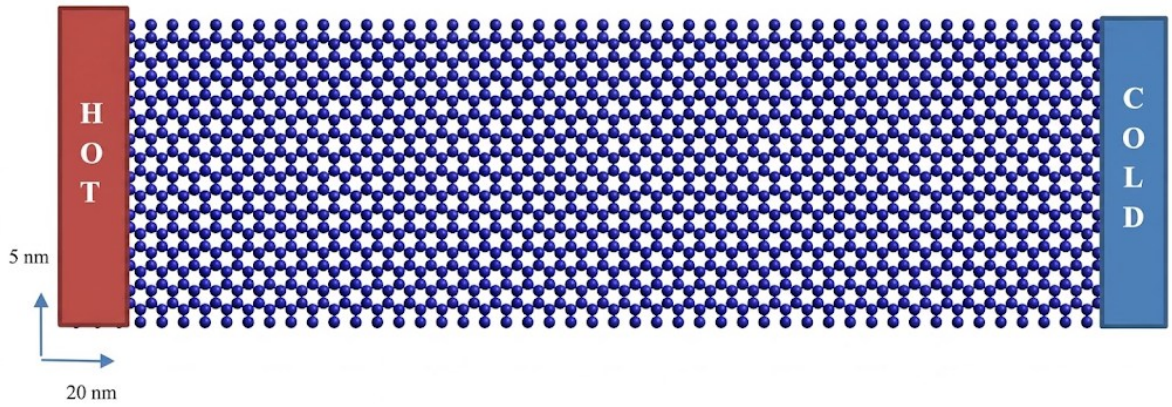


Figure 6. The imposed heat reservoir and heat sink in simulating the heat flux temperature profile of a silicene nanoribbon (blue color) with a length of 20 nm and a width of 5 nm.

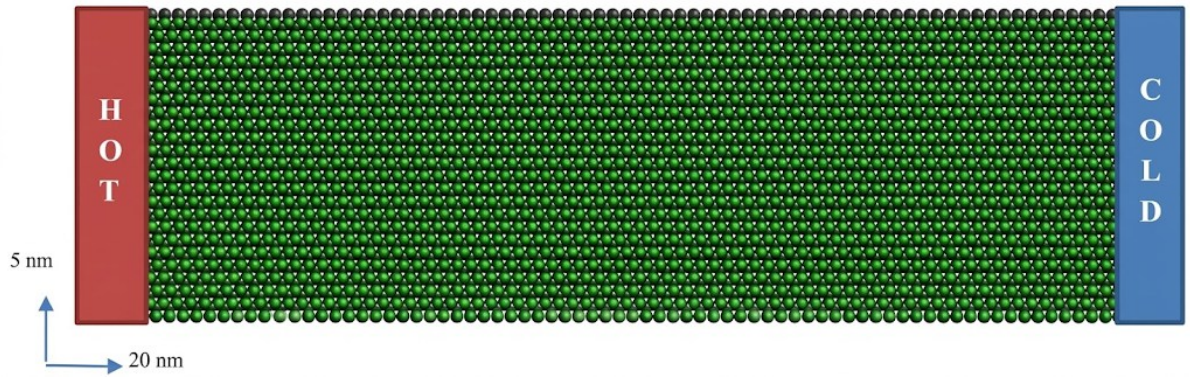
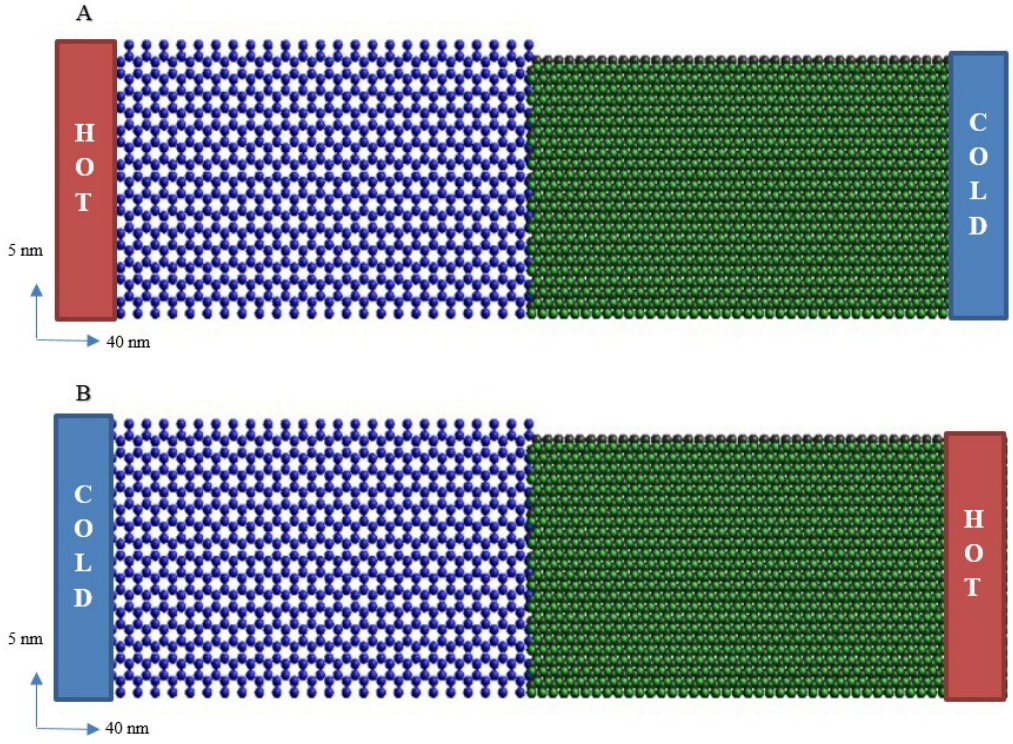


Figure 7. The imposed heat reservoir and heat sink in simulating the heat flux temperature profile of a graphane nanoribbon with a length of 20 nm and a width of 5 nm. Carbon atoms are shown in black, while hydrogen atoms are shown in green color.

©2026, Western Philippines University

In the silicene-graphane nanoribbons system, two configurations were created by reversing the positions of the heat reservoir and heat sink to simulate heat flow: one with the heat reservoir on the silicene (left) side and the heat sink on the graphane (right) side, and the other with the heat sink on the silicene side and the heat reservoir on the graphane side. This approach was used to examine the Kapitza resistance at the interface between silicene and graphane, as schematically shown in Figure 8. The nanoribbon dimensions were set to a length of 40 nm and a width of 5 nm. The system consisted of 1,632 silicon atoms, 3,936 carbon atoms, and 3,936 hydrogen atoms. Moreover, the silicene-graphane nanoribbons system was loaded from the restart file 2.a.1708000 with periodic boundaries (p p p), metal units, and atomic style. Atom groups were defined: Si (type 1), C (type 2), and H (type 3). Hot (x=0-30) and cold (x=371-401) slabs spanned y=0-50 (infinite z); the hot/cold were combined, excluding neighbors within a 2.0 Å. Heat flux was imposed along the x via fix heat (1.0/-1.0 eV/ps on the hot/cold), with NVE integration. Per-atom KE temperature T=KE/1.5kB (kB=8.617339e-5 eV/K) was spatially averaged (100/1000/100000 steps, x-bins of 10 lattice units, running average) into tempprofile.txt over 100,000 timesteps after the timestep reset. The hybrid potential consisted of Tersoff (SiC.tersoff for Si/C) and AIREBO (CH.airebo for C/H), with pair_coeff none for Si-H. Furthermore, the Kapitza resistance (R_k) was calculated as $R_k = \Delta T / q$, where ΔT is the temperature drop at the interface, and q is the magnitude of the heat flux (+-1.0 eV/ps). For the silicene-graphane nanoribbon (40 nm length × 5 nm width), q = 1.0 eV/ps converts to approximately 6.96×10^{10} W/m² using a cross-sectional area of 5 nm × 0.46 nm ($A = 2.3 \times 10^{-18}$ m²).



©2026, Western Philippines University

UNCORRECTED PROOF

Figure 8. The schematic model of silicene-graphane nanoribbons with heat baths. Silicon atoms are shown in blue. Hydrogen atoms are shown in green and are bonded to carbon atoms (shown in black) on both sides. (A) HOT and COLD heat baths; (B) COLD and HOT heat baths.

RESULTS

Thermal Conductivity of Silicene Nanoribbon and Graphane Nanoribbon

The thermal conductivity (κ) was calculated using the Green-Kubo method. Results indicate that at 300 K, the thermal conductivity of the silicene nanoribbon is 20.42 W/m·K, while that of the graphane nanoribbon is significantly higher at 1,592.89 W/m·K. This demonstrates that graphane nanoribbons possess much greater thermal conductivity than silicene nanoribbons. Furthermore, the temperature dependence of thermal conductivity for both materials reveals an increase in κ as the temperature rises from 50 K to 150 K, followed by a decrease in thermal conductivity at temperatures above 150 K, as shown in Figure 9.

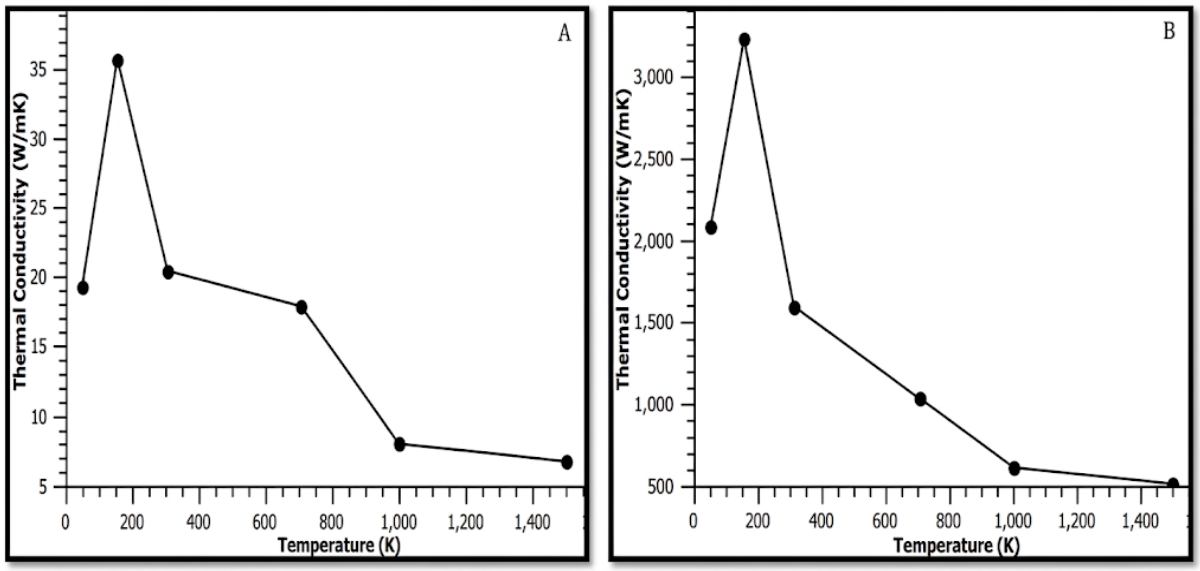


Figure 9. Thermal conductivity of (A) silicene nanoribbon as a function of temperature and (B) graphane nanoribbon as a function of temperature.

Heat Flux and Temperature Profile of Silicene Nanoribbon and Graphane Nanoribbon

In simulating the heat flux and temperature profiles of the silicene nanoribbon and graphane nanoribbon structures, heat reservoir (HOT) and heat sink (COLD) regions were established at the ends of the nanoribbons, each measuring 20 nm × 5 nm, as shown in Figure 10. A constant heat flux of 1.0 eV/ps was applied by adding this amount of energy per unit time to the HOT region and simultaneously removing the same amount from the COLD region, thereby imposing a controlled thermal gradient across the system. Results showed that, for silicene

UNCORRECTED PROOF

©2026, Western Philippines University

and graphane nanoribbons (20 nm length and 5 nm width) at 300 K, the temperature decreased progressively along their length as heat flux passed through, as depicted in Figure 10.

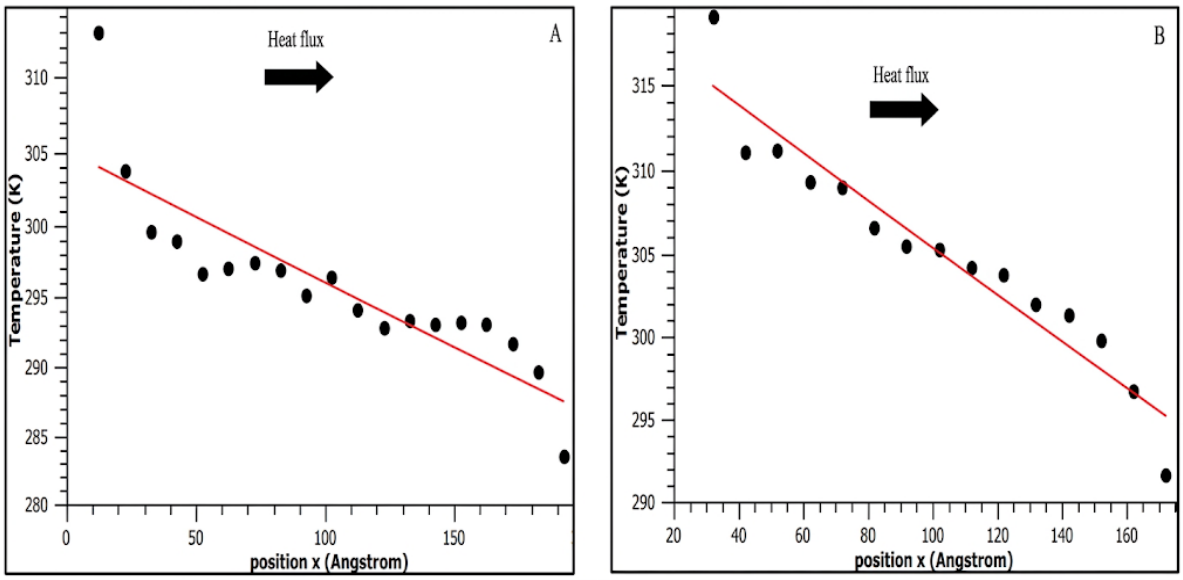
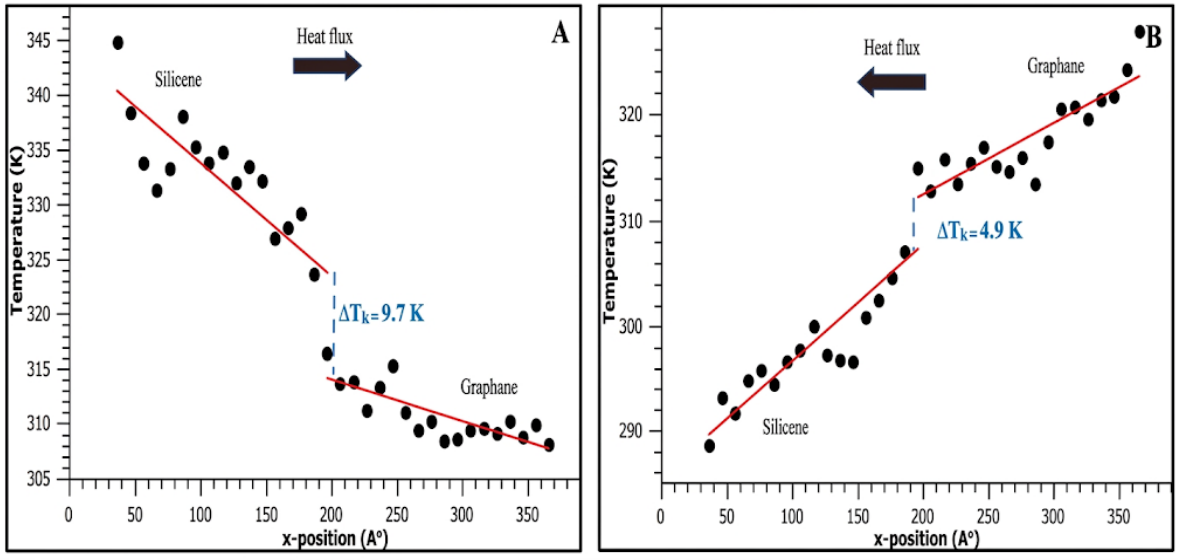


Figure 10. Heat flux and temperature profile of (A) silicene nanoribbon and (B) graphane nanoribbon.

Heat flux and Temperature Profile of Silicene-Graphane Nanoribbon

In simulating the heat flux and temperature profile of silicene-graphane nanoribbons with a length of 40 nm and a width of 5 nm, a heat reservoir and heat sink were also put in place to establish heat flux. Moreover, to investigate the presence of Kapitza resistance, the HOT and COLD regions were interchanged, creating two heat flux directions: one from left to right and the other from right to left (as shown in Figure 11). The results illustrate the heat flux flowing through the crystal lattice of the silicene-graphane nanoribbons system, demonstrating that heat transfer occurs bidirectionally between silicene and graphane.



©2026, Western Philippines University

Figure 11. Temperature profile for heat flux in (A) the positive (+) direction of the silicene-graphane nanoribbon and (B) the negative (-) direction of the silicene-graphane nanoribbon.

DISCUSSION

Thermal Conductivity of Silicene Nanoribbon and Graphane Nanoribbon

The thermal conductivity of the graphane nanoribbon is significantly higher than that of the silicene nanoribbon. This may be attributed to the high thermal conductivity of graphene, from which graphane is derived, highlighting a substantial variation in their heat conduction behaviors. In addition, graphane displays significantly reduced thermal conductivity compared to graphene due to hydrogenation, which induces sp^3 hybridization, disrupts π bonding, and introduces buckling that enhances phonon scattering via localized modes and acoustic branch softening (Dehaghani et al. 2022). In graphane, hydrogenation increases Umklapp scattering rates (2–5 × higher than graphene) and lowers phonon group velocities (e.g., ZA mode with a reduction of approximately 20–30%), typically yielding κ values well below graphene's 2000–5000 W/m·K at 300 K (Gu and Yang 2015). However, the Green–Kubo thermal conductivity obtained for the simulated graphane structure, 1,592.89 W/m·K, is unexpectedly high because hydrogenation generally suppresses the thermal transport of graphene through changes in bonding and phonon scattering. First-principles phonon-transport calculations indicate that hydrogenation reduces graphene thermal conductivity, whereas pristine graphene itself commonly exhibits room-temperature values in the several-thousand-W/m·K range (Ghosh et al. 2009; Fugallo et al. 2014). The calculated value nevertheless remains substantially greater than typical predictions for silicene, which are commonly near 20–30 W/m·K (Xie et al. 2014; Wang et al. 2015). This discrepancy may reflect finite-size effects, model geometry or edge effects if a nanoribbon was simulated, incomplete hydrogenation or residual sp^2 domains, the interatomic potential employed, thickness/volume assumptions for the two-dimensional material, or incomplete convergence of the heat-current autocorrelation-function integral. Green–Kubo conductivity is obtained by integrating the heat-current autocorrelation function, so convergence should be demonstrated through running-integral plateaus, multiple independent trajectories, and uncertainty estimates rather than by applying a fixed simulation-time threshold (Wang 2014). Moreover, limitations of classical force fields such as Tersoff/AIREBO often overestimate κ by underestimating anharmonic C-H scattering, unlike machine-learned interatomic potentials (MLIPs) or density functional theory-trained (DFT) potentials that better capture sp^3 phonons (Li and Yang 2012). Furthermore, as seen in Figure 9, the silicene and graphane nanoribbons, with fixed lengths of 20nm and widths of 5nm, exhibited an increase in thermal conductivity as the temperature increased from 50 K to 150 K due to the harmonic

UNCORRECTED PROOF

©2026, Western Philippines University

oscillations of the atoms, which affect the movement and heat transfer in the material (Che et al. 2000; Hu et al. 2009). At low temperatures, thermal conductivity increases with temperature, following a T^3 relationship. This is because the heat capacity of the material increases rapidly with temperature, while the distance phonons travel between collisions (the mean free path) stays roughly the same. On the other hand, temperatures above 150 K show the occurrence of anharmonic oscillations of the atoms that lead to phonon-phonon scattering, which causes the continuing drop of thermal conductivity (Hu et al. 2009; Rangrajan 2026). Moreover, at high temperatures, thermal conductivity decreases as temperature rises. In this range, the heat capacity remains constant, but phonons—responsible for carrying heat—scatter more frequently due to Umklapp processes, which limit their ability to transport heat efficiently. Hence, the mean free path has an inverse relation to temperature, and the thermal conductivity decreases (Nika et al. 2009; Hepplestone and Srivastava 2010; Li and Yang 2012).

Heat Flux and Temperature Profile of Silicene Nanoribbon and Graphane Nanoribbon

The thermostats imposed at the edges of the silicene and graphane systems cause phonon scattering, which limits the phonon mean free path, causing a decrease in temperature (Mu et al. 2014). Furthermore, the temperature decreases steadily from left to right, indicating the direction of heat flow (as marked by the arrow) shown in Figure 10. The red line closely follows the trend of the data points, demonstrating that the temperature profile is approximately linear across the nanoribbons. This linearity signifies that a steady-state heat flow has been established, with a uniform temperature gradient resulting from the constant heat flux imposed on the system (Plimpton 1995).

Heat flux and Temperature Profile of Silicene-Graphane Nanoribbon

When heat flux is applied to the silicene-graphane system, lattice vibrations occur at the interface causing the lattice to stretch due to the lattice mismatch. The lattice mismatch at the interface causes a dislocation (Hepplestone and Srivastava 2010) which increases the lattice disorder (Li and Yang 2012), leading to phonon scattering. Furthermore, when phonons are transported across the interface between materials, they undergo reflection, transmission, and mode conversion, which lead to a local temperature jump at the interface (Li and Yang 2012). Alternatively, phonon scattering at the interface can cause an abrupt temperature drop, a phenomenon known as the Kapitza effect (Rajabpour et al. 2011). The observed local temperature drops were 9.7 K and 4.9 K for positive and negative heat flux directions, respectively, demonstrating a pronounced directional dependence of interfacial thermal resistance, as shown in Figure 11. Silicene-graphane nanoribbons exhibit a nonsymmetric

©2026, Western Philippines University

UNCORRECTED PROOF

temperature gradient due to the hybrid sp^2-sp^3 bonding: silicene's buckled lattice (Si atoms) promotes out-of-plane flexural phonons with higher scattering rates on one side, as reported in the study of silicene-graphene nanoribbon (Zhou et al. 2022), while graphane's fully hydrogenated, planar structure (sp^3 C-H bonds) enhances in-plane acoustic phonon transport on the other. This leads to a steeper drop (9.7 K) along the silicene-dominated direction due to stronger anharmonic Umklapp scattering and mass mismatch at the interface, reducing the mean free path. The shallower 4.9 K drop occurs bidirectionally along the graphane edge, where hydrogenation stiffens bonds, lowering the flexural phonon density of states and preserving longer phonon lifetimes—yielding approximately 50% higher thermal conductivity at 300 K compared to pure silicene. In addition, the Kapitza resistance (R_k) is calculated as $R_k = \Delta T / q$, where ΔT is the temperature drop at the interface, and q is the magnitude of the heat flux ($\pm$ 1.0 eV/ps). For the silicene-graphane nanoribbon (40 nm length and 5 nm width), q = 1.0 eV/ps converts to approximately 6.96×10^{10} W/m^2 using a cross-sectional area of 5 nm × 0.46 nm (graphane thickness) ($A = 2.3 \times 10^{-18}$ m^2). Thus, the Kapitza resistance values are 1.39×10^{-10} m^{2}K/W for ΔT = 9.7 K and 7.04×10^{-11} m^{2}K/W for ΔT = 4.9 K. These values were consistent with Kapitza resistances for 2D heterostructure interfaces (~10^{-10} to 10^{-9} m^{2}K/W) (Chen et al. 2020), reflecting phonon mismatch in the 40 nm × 5 nm system under NEMD steady-state conditions with bidirectional flux (±1.0 eV/ps). Moreover, this ~2:1 ratio stems from phonon mismatch due to silicene's buckled Si-C structure (weaker bonds ~2.3 eV, buckling 0.47 Å) versus graphane's flat C-H structure (stronger bonds of ~4.3 eV), where the atomic mass contrast (Si 28 u vs. H 1 u), bonding strength asymmetry, and effective interface roughness from structural disparity amplify scattering in the forward direction while aiding transmission in the reverse direction, as seen in Figure 11. These findings provide critical insights into the anisotropic thermal transport behavior of hybrid silicene-graphane nanoribbons, underscoring their potential for tailored thermal management in advanced nanodevices (Kim et al. 2021; Song et al. 2022).

In conclusion, this study provides a detailed analysis of the thermal transport properties of silicene-graphane nanoribbons through non-equilibrium molecular dynamics simulations. The thermal conductivities of silicene and graphane nanoribbons were quantified using the Green-Kubo formalism, revealing a significant contrast at room temperature—20.42 W/m·K for silicene and 1,592.89 W/m·K for graphane. The temperature-dependent behavior showed a decrease in thermal conductivity with rising temperature, driven by enhanced phonon-phonon scattering due to anharmonic atomic vibrations. At low temperatures, thermal conductivity increased following a T^3 trend, dominated by heat capacity effects with a constant phonon mean free path. At

©2026, Western Philippines University

UNCORRECTED PROOF

higher temperatures, saturation of heat capacity and Umklapp scattering reduced the phonon mean free path, leading to decreased thermal conductivity. The study also highlighted the Kapitza resistance at the silicene-graphane interface, with values of 1.39×10^{-10} m^2·K/W for $\Delta T = 9.7$ K and 7.04×10^{-11} m^2·K/W for $\Delta T = 4.9$ K. These values were consistent with Kapitza resistances for 2D heterostructure interfaces (~10^{-10} to 10^{-9} m^2·K/W) (Chen et al. 2020), reflecting phonon mismatch in the 40 nm × 5 nm system under NEMD steady-state conditions with bidirectional flux (±1.0 eV/ps). Importantly, this interfacial thermal resistance exhibited directional dependence, underscoring anisotropic heat transport behavior. These insights deepen the understanding of thermal phenomena in hybrid nanoribbons and underscore their potential for engineered thermal management in future nanoscale devices. Future improvements could enhance accuracy, extend the scope, and bridge simulations to experiments for silicene-graphane nanoribbons. The researchers recommend replacing classical MD potentials (e.g., AIREBO) with MLIPs trained on DFT data or incorporating quantum statistics via ring-polymer MD to better capture anharmonic C-H/Si vibrations, especially in light of graphane's unexpectedly high thermal conductivity of 1592.89 W/m·K—potentially resolving classical overestimation of long-wavelength phonons. They also recommend testing larger supercells (>100 nm) and varied widths to quantify finite-size effects on the T^3 low-T trend and Umklapp regime; including edge passivation (H-termination) to isolate boundary scattering from bulk properties; expanding the Kapitza resistance analysis (1.39×10^{-10} to 7.04×10^{-11} m^{2}K/W) with phonon transmission spectra via atomic Green's function methids or Boltzmann Transport Equation solvers, validating NEMD anisotropy against ΔT dependence. Finally, they recommend simulating doping, vacancies, or biaxial strain to tune interface resistance below 10^{-10} m^2·K/W, targeting thermal diodes/rectifiers for nanoelectronics.

FUNDING

This research received no internal or external funding.

GENERATIVE AI STATEMENT

During the preparation of this manuscript, the authors used generative artificial intelligence (AI) tools solely to assist with initial literature searches, source identification, and language refinement (improving grammar, readability, and clarity). All scientific conceptualization, C/C++ lattice construction in Code::Blocks, 3D structural validation in HyperChem, classical non-equilibrium molecular dynamics (NEMD) simulations in LAMMPS, and thermal transport analyses were conducted entirely by the authors. After using these AI tools, the authors

©2026, Western Philippines University

UNCORRECTED PROOF

independently verified all referenced sources, thoroughly reviewed and edited the text, and take full responsibility for the accuracy, originality, and integrity of the published work.

ETHICAL CONSIDERATIONS

This research was purely computational, using molecular dynamics simulations to examine thermal transport in silicene, graphane, and hybrid silicene-graphane nanoribbons. As the study did not involve human participants, animal subjects, or biological materials, ethics committee approval was not applicable. All simulation procedures, software tools (Code::Blocks, HyperChem, and LAMMPS), and findings were executed and reported with full academic integrity and proper attribution using institutional computing resources from the Department of Physics, Mindanao State University – Iligan Institute of Technology.

DECLARATION OF COMPETING INTEREST

The authors declare that they have no competing interests.

ACKNOWLEDGMENTS

Gratitude is extended to the Department of Physics, MSU–Iligan Institute of Technology, for providing access to advanced computing facilities, which were instrumental in conducting this research. The department's support provided the computational resources needed to complete the study. The authors also sincerely thank the anonymous reviewers for their valuable comments and constructive suggestions, which contributed to improving the quality and clarity of this manuscript.

REFERENCES

Che J, Cagin T, Goddard WA III. 2000. Thermal conductivity of carbon nanotubes. Nanotechnology. 11(2):65–69. https://doi.org/10.1088/0957-4484/11/2/305

Chen X-K, Zeng Y-J, Chen K-Q. 2020. Thermal transport in two-dimensional heterostructures. Frontiers in Materials. 7:578791. https://doi.org/10.3389/fmats.2020.578791

CCCBD (Computational Chemistry Comparison and Benchmark Database). 2022. Standard Reference Database 101. National Institute of Standards and Technology. [accessed 2026 Sep 03]. https://cccbdb.nist.gov/calcbondcomp3x.asp?i=14&j=14&mi=90&bi=10.

Dehaghani MZ, Habibzadeh S, Farzadian O, Kostas KV, Saeb MR, Spitas C, Mashhadzadeh AH. 2022. Heat transfer through hydrogenated graphene superlattice nanoribbons: a computational study. Scientific Reports. 12:7966. https://doi.org/10.1038/s41598-022-12168-7

Ghosh S, Nika DL, Pokatilov EP, Balandin AA. 2009. Heat conduction in graphene: Experimental study and theoretical interpretation. New Journal of Physics. 11(9):095012. https://doi.org/10.1088/1367-2630/11/9/095012

Gu X, Yang R. 2015. First-principles prediction of phononic thermal conductivity of silicene: a comparison with graphene. Journal of Applied Physics. 117:025102. https://doi.org/10.1063/1.4905540

Grazianetti C, Molle A, Martella C. 2023. Silicene applications in nanotechnology: from transistors to bendable membranes. TechRxiv. 2023(1202). https://doi.org/10.36227/techrxiv.24631008.v1

Gordiz K, Vaez Allaei SM, Kowsary F. 2011. Thermal rectification in multi-walled carbon nanotubes: A molecular dynamics study. Applied Physics Letters. 99(25):251901.https://doi.org/10.1063/1.3670327

Fiveable. 2026. 2.1 One-Dimensional Steady-State Conduction – Heat and Mass Transfer. [accessed 2026 Aug 27]. https://fiveable.me/key-terms/heat-mass-transfer/steady-state-conduction.

Fugallo G, Lazzeri M, Paulatto L, Mauri F. 2014. Thermal conductivity of graphene and graphite: Collective excitations and mean free paths. Nano Letters. 14(11):6109–6114. https://doi.org/10.1021/nl502059f

Hepplestone SP, Srivastava GP. 2010. Theory of interface scattering of phonons in superlattices. Physical Review B. 82(14):144303. https://doi.org/10.1103/PhysRevB.82.144303

Hu J, Ruan X, Jiang Z, Chen YP. 2009. Thermal conductivity and thermal rectification in graphene nanoribbons: a molecular dynamics study. Nano Letters. 9(7):2730-2735. https://doi.org/10.1021/nl901231s

Hypercube Inc. 2007. Hypercube Inc. Scientific Software. [accessed 2026 Sep 03]. http://www.hypercubeusa.com/

©2026, Western Philippines University

UNCORRECTED PROOF

Kim SE, Mujid F, Rai A, Eriksson F, Suh J, Poddar P, Ray A, Park C, Fransson E, Zhong Y, and others. 2021. Extremely anisotropic van der Waals thermal conductors. Nature. 597(7878):660–665. https://doi.org/10.1038/s41586-021-03867-8

Li F, Tang X, Fei Y, Zhang J, Liu J, Lang P, Che G, Zhao Z, Zheng Y, Fang Y, and others. 2025. Ordered graphane nanoribbons synthesized via high-pressure Diels–Alder polymerization of 2,2′-bipyrazine. Journal of the American Chemical Society. 147(17):14054–14059. https://doi.org/10.1021/jacs.5c03116

Li X, Yang R. 2012. Effect of lattice mismatch on phonon transmission and interface thermal conductance across dissimilar material interfaces. Physical Review B. 86:054305. https://doi.org/10.1103/PhysRevB.86.054305

Mbayachi VB, Ndayiragije E, Sammani T, Taj S, Mbuta E, Khan A. 2021. Graphene synthesis, characterization and its applications: A review. Results in Chemistry. 3:100163. https://doi.org/10.1016/j.rechem.2021.100163

Mu X, Wu X, Teng Z, Go D, Luo T. 2014. Thermal transport in graphene oxide—from ballistic extreme to amorphous limit. Scientific Reports. 4:3909. https://doi.org/10.1038/srep03909

NTESS (National Technology and Engineering Solutions of Sandia). 2025. LAMMPS molecular dynamics simulator. [accessed 2025 Sep 03]. http://lammps.sandia.gov.

Nika DL, Pokatilov EP, Askerov AS, Balandin AA. 2009. Phonon thermal conduction in graphene: role of Umklapp and edge roughness scattering. Physical Review B. 79:155413. https://doi.org/10.1103/PhysRevB.79.155413

Plimpton S. 1995. Fast parallel algorithms for short-range molecular dynamics. Journal of Computional Physics. 117(1):1-19. https://doi.org/10.1006/jcph.1995.1039

Rajabpour A, VaezAllaei SM, Kowsary F. 2011. Interface thermal resistance and thermal rectification in hybrid graphene–graphane nanoribbons: a nonequilibrium molecular dynamics study. Applied Physics Letters. 99:051917. https://doi.org/10.1063/1.3622480

Rangrajan G. 2026. Condensed matter physics: lecture 14 - lattice vibrations (cont.), phonon thermal conductivity (video lecture). Infocobuild. [accessed 2026 Aug 27]. http://www.infocobuild.com/education/audio-video-courses/physics/CondensedMatterPhysics-IIT-Madras/lecture-14.html.

Roberts NA, Walker DG. 2011. A review of thermal rectification observations and models in solid materials. International Journal of Thermal Sciences. 50(5):648-662. https://doi.org/10.1016/j.ijthermalsci.2010.12.004

Shrestha R, Luan Y, Luo X, Shin S, Zhang T, Smith P, Gong W, Bockstaller M, Luo T, Chen R, and others. 2020. Dual-mode solid-state thermal rectification. Nature Communications. 11(1):4346. https://doi.org/10.1038/s41467-020-18212-2

Singh AK, Yakobson BI. 2009. Electronics and Magnetism of Patterned Graphene Nanoroads. Nano Letters. 9(4):1540-1543. https://doi.org/10.1021/nl803622c

Sofo JO, Chaudhari AS, Barber GD. 2007. Graphane: a two-dimensional hydrocarbon. Physics Review B. 75:153401. https://doi.org/10.1103/PhysRevB.75.153401

Song X, Zhang Y, Jun N, Sheng M, Zhenhong D. 2022. Thermal transport properties of anisotropic materials RbCaX (X = As, Sb) with strong anharmonicity. Computational Materials Science. 213:111618. https://doi.org/10.1016/j.commatsci.2022.111618

Topsakal M, Cahangirov S, Ciraci S. 2010. The response of mechanical and electronic properties of graphane to the elastic strain. Applied Physics Letters. 96(9):091912. https://doi.org/10.1063/1.3353968

Tsai W, Huang C, Chong T, Lin H, Horng T, Bansil A. 2013. Gated silicene as a tunable source of nearly 100% spin-polarized electrons. Nature Communication. 4:1500. https://doi.org/10.1038/ncomms2525

Wang Y, Vallabhaneni AK, Qiu B, Ruan X. 2014. Two-dimensional thermal transport in graphene: a review of numerical modeling studies. Nanoscale and Microscale Thermophysical Engineering. 18:155-182. https://doi.org/10.1080/15567265.2014.891680

Wang Z, Xie R, Broido DA. 2015. Thermal conductivity and spectral phonon properties of freestanding and supported silicene. Physical Review B. 91(23):235415. https://doi.org/10.1103/PhysRevB.91.235415

Wu B, Yang C. 2012. Electronic structures of graphane with vacancies and graphene adsorbed with fluorine atoms. AIP Advances. 2(1):012173. https://doi.org/10.1063/1.3696883

Xiang-Tao A, Zhang Y, Liu J, Li S. 2013. Quantum spin Hall effect induced by electric field in silicene. Applied Physics Letters. 102:043113. https://doi.org/10.48550/arXiv.1212.4577

Xie H, Ouyang T, Germaneau E, Chen G. 2014. Thermal conductivity of silicene calculated using an optimized Stillinger–Weber potential. Physical Review B. 89(5):054310. https://doi.org/10.1103/PhysRevB.89.054310

Zhang X, Hu M, Tang D. 2013. Thermal rectification at silicon/horizontally aligned carbon nanotube interfaces. Journal of Applied Physics. 113:194307. https://doi.org/10.1063/1.4804071

Zhong Y 2021. Understanding and characterizing thermal transport in 2D van der Waals nanoelectronics. Massachusetts Institute of Technology. [accessed 2026 Sep 4]. https://hdl.handle.net/1721.1/140144

Zhou J, Li H, Tang H-K, Shao L, Han K, Shen X. 2022. Phonon Thermal Transport in Silicene/Graphene HeterobilayerNanostructures: Effect of Interlayer Interactions. ACS Omega. 7(7):5844–5852. https://doi.org/10.1021/acsomega.1c05932

ROLE OF AUTHORS: MTB *– conceptualization, original proposal and final manuscript writing, and investigation, simulations, and data analysis;* ***GJP*** *– conceptualization, methodology, data analysis, supervision, reviewing, and editing.*

Responsible Editor: Dr. Hector R. Lim, Jr.

UNCORRECTED PROOF

©2026, Western Philippines University